ANNUAL REVIEWS

Annual Review of Physical Chemistry

Dry Deposition of Atmospheric Aerosols: Approaches, Observations, and Mechanisms

Delphine K. Farmer, Erin K. Boedicker, and Holly M. DeBolt

Department of Chemistry, Colorado State University, Fort Collins, Colorado 80523, USA; email: delphine.farmer@colostate.edu

Annu. Rev. Phys. Chem. 2021. 72:375–97

First published as a Review in Advance on January 20, 2021

The *Annual Review of Physical Chemistry* is online at physchem.annualreviews.org

https://doi.org/10.1146/annurev-physchem-090519-034936

Keywords

aerosol, particle, dry deposition, flux

Abstract

Aerosols are liquid or solid particles suspended in the atmosphere, typically with diameters on the order of nanometers to microns. These particles impact air quality and the radiative balance of the planet. Dry deposition is a key process for the removal of aerosols from the atmosphere and plays an important role in controlling the lifetime of atmospheric aerosols. Dry deposition is driven by turbulence and shows a strong dependence on particle size. This review summarizes the mechanisms behind aerosol dry deposition, including measurement approaches, field observations, and modeling studies. We identify several gaps in the literature, including deposition over the cryosphere (i.e., snow and ice surfaces) and the ocean; in addition, we highlight new techniques to measure black carbon fluxes. While recent advances in aerosol instrumentation have enhanced our understanding of aerosol sources and chemistry, dry deposition and other loss processes remain poorly investigated.

1. INTRODUCTION

Aerosols are the strongest drivers of uncertainties in understanding human impacts on climate (1, 2). Aerosols are small particles, either liquid or solid, suspended in the atmosphere. These particles directly interact with light through scattering (thereby having a cooling impact in the atmosphere, the extent of which depends on particle size) and absorption (thereby warming the atmosphere if the particle composition has adequate chromophores, typically through so-called brown and black carbon). However, particles can also have indirect impacts on the atmosphere's radiative balance by their interactions with water vapor in the atmosphere and growth into cloud droplets. Cloud droplets scatter light and enhance the albedo of the planet, and anthropogenic particles tend to enhance the albedo of clouds. The physical size and chemical properties of atmospheric aerosol particles determine their potential to influence the radiative balance of the planet. These properties are not static: Atmospheric chemistry can change the chemical and physical properties of aerosol particles. Gas-particle partitioning, coagulation with other particles, and chemical reactions on particle surfaces can all enable changes in composition and chemical properties, including hygroscopicity, volatility, and viscosity. All of the different ways that aerosols affect climate, however, depend on their concentrations, which in turn depend strongly on their removal rates. Thus, while these aerosol–cloud–radiation interactions are complex, it is the removal of these particles from the atmosphere that represents the single largest uncertainty in climate (3, 4). Here, we build on previous work (5–8) and review the literature on the dry deposition of particles from the atmosphere to surfaces, with particular emphasis on particle deposition measurements in the submicron size range over different surface types.

1.1. Particle Lifetime

Particles are removed from the atmosphere through wet and dry deposition, both of which are typically considered true sinks (**Figure 1**). Dry deposition refers to the removal of particles by collision with terrestrial or hydrological surfaces by gravitational settling, impaction,

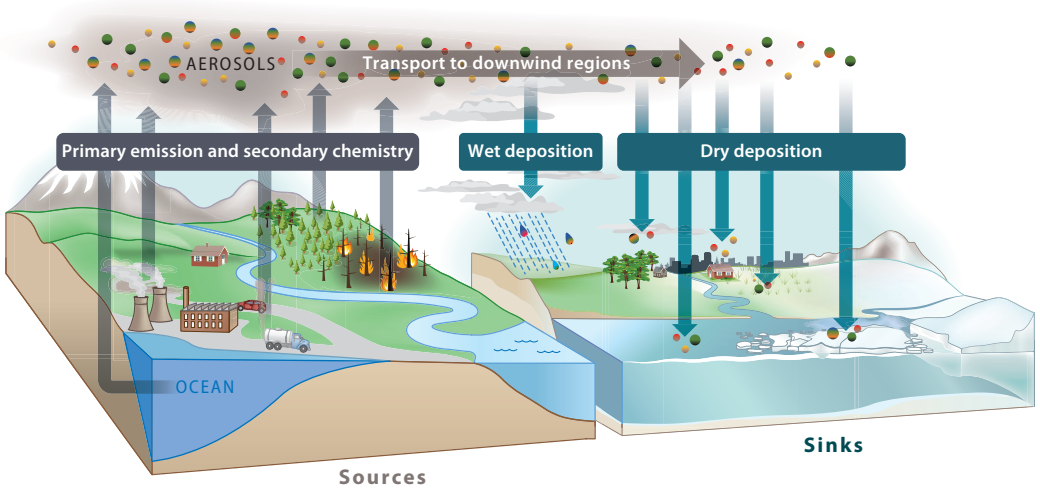

Figure 1

Primary emissions and secondary chemistry are key sources of aerosols in the atmosphere. Wet and dry deposition remove particles, determining the lifetime of these aerosols in the atmosphere. Deposition surfaces include forests, grasslands, ice, water, and urban environments, with each surface type removing particles at different size- and turbulence-dependent rates.

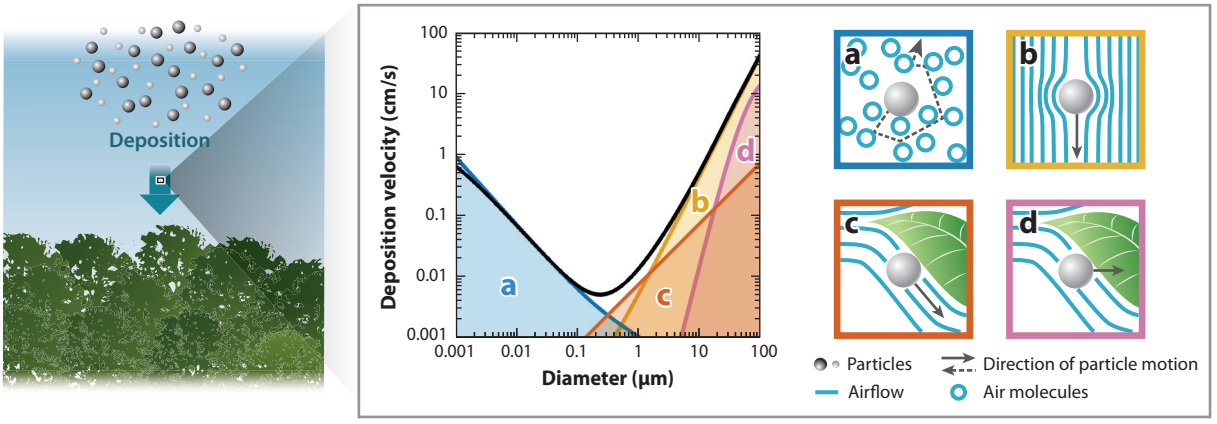

Figure 2

Dry deposition velocities of particles are a function of particle diameter and are driven by a combination of processes, including (*a*) Brownian diffusion (*blue*), (*b*) gravitational settling (*yellow*), (*c*) interception (*orange*), and (*d*) impaction (*purple*). The relative importance of these processes varies with particle size and surface type, with the graph providing an example of these processes and the total calculated deposition velocity (*thick black line*) for a conifer forest. The direction of airflow in panels *a–d* is indicated by solid blue lines; the direction of particle motion is indicated by gray arrows. In the case of Brownian diffusion, particle movement is random, as indicated by the dashed gray arrow. The size of particles relative to gases is not drawn to scale.

interception, and/or diffusion (**Figure 2**). Wet deposition refers to the scavenging of particles from the atmosphere by solid or liquid water and their subsequent removal by precipitation. One nuance in this definition of wet deposition is that cloud droplets can subsequently evaporate and release the particles back into the atmosphere, albeit after potentially substantial aqueous chemical processing. As a result of wet and dry deposition, the lifetime of submicron particles is typically considered to be about a week in the atmosphere, which is long enough for intercontinental transport. On a global scale, this lifetime is dominated by wet deposition, but dry deposition is an important lever on aerosol lifetime in the absence of precipitation.

There are serious problems with our current understanding of deposition rates: Current parameterizations are inaccurate (9–14); measurements are scarce; and, as expected, the rates are very important. For example, Goldstein & Galbally (15) estimated that wet deposition of secondary organic aerosols (one type of aerosol) was about four times that of dry deposition, but that the uncertainties in organic aerosol lifetimes due to deposition were substantial. As the atmospheric relevance of aerosol-phase reactions is often assessed by a comparison of reaction rates versus aerosol lifetimes, this uncertainty in deposition rates also impacts the way we think about aerosol chemical reactivity.

The relative importance of these dry deposition processes depends on particle size, with gravitational settling significantly impacting only larger (i.e., >10 μm in diameter) particles and diffusion acting on only smaller (<300 nm) particles (16). Dry deposition is typically described by the concentration (C) of the species of interest and a deposition velocity, V_{dep}:

$$\text{Deposition flux} = -V_{dep} \times C. \quad 1.$$

V_{dep} is expressed as a rate; for submicron aerosol particles, V_{dep} is typically on the order of 0.1 cm/s. A downward flux, or deposition, is taken as a negative flux by convention, while an upward or emitting flux is positive. V_{dep} provides a particularly useful metric for comparing results across sites—and for modeling particle removal—because it is independent of ambient concentration. Observation techniques typically measure the flux and concentration of particles and derive the

V_{dep}. However, dry deposition is challenging to measure because most measurement techniques rely on micrometeorological techniques, which require careful site selection and either vertical gradients in concentration (difficult to achieve as differences in actual concentration may be on par with or smaller than differences in inlet losses) or particularly fast, sensitive, and selective detectors for eddy covariance (EC) flux measurement (Section 2).

The V_{dep} of particles can be directly related to the lifetime of aerosols due to dry deposition:

$$\tau_{\text{dry dep}} = \frac{V_{\text{dep}}}{\text{BLH}}, \qquad 2.$$

where BLH is the boundary layer height (typical afternoon BLH values in the troposphere are from 1 to 3 km). The total atmospheric lifetimes of particles are determined by both dry and wet deposition. However, atmospheric chemists rarely consider total particle concentration and instead often consider particles of specific sizes. In these cases, the lifetimes of particles additionally depend on their removal rates from the size range of interest through coagulation or condensation (resulting in particle growth). Particles are less likely to shatter in the atmosphere, though particles can shrink due to evaporation.

1.2. Particle Deposition as a Key Uncertainty in Climate Models

While there are many reasons for the uncertainty about the impact of aerosols on climate, it fundamentally stems from the challenges in representing the processes that shape the size and concentration of particles in the atmosphere, including aerosol sources and sinks. Lee et al. (4) found uncertainty in dry deposition velocities of particles in the accumulation mode to be the largest contributor to uncertainty in cloud condensation nuclei (CCN) concentration in global models, which is critical to understanding cloud interactions (4). CCN are the particles into which water vapor condenses in the atmosphere and that form cloud droplets. CCN can have varying compositions and sources, and we point the reader to several reviews that summarize the chemistry and physics of CCN (17, 18). CCN are typically submicron in diameter, but the deposition rates of larger particles are also relevant to climate processes, including dust (100 nm to 100 μm in size) CCN. Similarly, Carslaw et al. (2) found the dry deposition of accumulation mode particles to be the largest contributor to uncertainties in the cloud albedo aerosol indirect effect.

Dry deposition parameterizations are important to get right. Lee et al. (4) used expert elicitation to determine plausible ranges for 28 uncertain inputs to global aerosol microphysics models, including dry deposition of Aitken (0.01–0.1 μm in diameter) and accumulation mode (typically 0.1–1 μm in diameter) particles. The purpose of this study was to determine the model inputs that contribute most to uncertainties in CCN predictions both globally and regionally. Lee et al. (4) found the dry deposition of particles in the accumulation mode to be the largest individual contributor to uncertainty in CCN, and Aitken mode dry deposition to be the ninth most important contributor. The maximum absolute uncertainties in CCN due to dry deposition occur over land where aerosol concentrations are highest. The maximum relative CCN uncertainties occur over remote regions and are due to instances in which dry deposition is the sole removal mechanism for air masses over timescales of several days. Uncertainties in size-dependent aerosol dry deposition rates dominate CCN prediction uncertainties over remote regions, particularly in regions with low precipitation rates.

In a parallel study, Carslaw et al. (2) found the dry deposition of accumulation mode particles to be the largest aerosol process contributor to uncertainties in the cloud albedo aerosol indirect effect. The bounding range for Aitken mode aerosol deposition was 0.5–2 times the best guess (scaled evenly around the globe), while the bounding range for accumulation mode deposition

was 0.1–10 times the best-guess values. These uncertainty ranges reflect uncertainties in both the dry deposition parameterizations themselves (16, 19) and the uncertainties in the variability of sub-grid-scale deposition rates. The large uncertainty range for the accumulation mode particles is due to the more parameterized nature of the deposition of these particles as opposed to the relatively well-understood Brownian diffusion of the smaller Aitken mode particles (20).

The results of Carslaw et al. (2) and Lee et al. (4) strongly emphasize the need for increased certainty in accumulation mode aerosol dry deposition rates. The spatial distribution of these relative CCN uncertainties (proportional to aerosol indirect effect uncertainties) is particularly intriguing. Remote ocean surfaces also remain among the most logistically challenging environments over which to conduct field measurements. Further, measurements over water surfaces are inherently challenged by the competition between deposition processes and the simultaneous emission of sea spray aerosol due to wave breaking.

1.3. Particles as a Source of Nutrients and Pollutants to Ecosystems

While wet and dry deposition processes obviously remove particles from the atmosphere, mass is conserved: These processes, which act as sinks from the atmosphere, are also sources to Earth's terrestrial and aquatic surfaces. The addition of acidic compounds, including sulfuric acid or sulfate ions and nitric acid or nitrate ions, has been the focus of decades of research into acid deposition to ecosystems. The addition of such components through atmospheric deposition can have devastating consequences to ecosystems including shifts in biodiversity, diminished plant health, and damage to aquatic life (21). The deposition of nitrogen compounds has been an additional focus in terrestrial ecosystems, as nitrogen is often a limiting nutrient in temperate forests and agricultural systems (22). Aerosols are often an important source of this deposition to natural ecosystems, although their impact on crops is potentially small (23). For example, one study in the Netherlands (24) suggested that aerosol deposition accounts for 9% of total nitrate (NO_3^-) and 11% of ammonium (NH_4^+) deposition over the entire country; however, the relative contribution of aerosols approximately doubled over forests, accounting for 20% of NO_3^- and 17% of NH_4^+ deposition over coniferous forests. Phosphorus is an intriguing element in terms of aerosol deposition: While there are few measurements of aerosol phosphate deposition, Vicars et al. (25) showed that the deposition of aerosol phosphorus was significant to ecosystems in the Sierra Nevada, potentially leading to phytoplankton growth and eutrophication in lakes. We point readers to a recent review by Bobbink et al. (26) for a detailed analysis of long-term trends and consequences of atmospheric deposition from an ecosystem perspective. The deposition of particles containing toxic metals, pesticides, polyflourinated compounds, or persistent organic pollutants is an emerging topic of concern (27–29). Thus, a mechanistic understanding of particle deposition is essential not only for understanding the lifetimes of aerosols in the atmosphere but also for determining the addition of pollutants and nutrients from the atmosphere to terrestrial and aquatic ecosystems.

2. APPROACHES TO MEASURING PARTICLE DEPOSITION

Our capacity to accurately parameterize dry deposition and thus model particle lifetimes in the atmosphere is limited by the small number of observations of particle fluxes. While measuring particle number concentrations, size distributions, and composition is relatively straightforward (30), flux measurements are not. Measurements of the surface–atmosphere exchange of particles—particularly in remote, low-concentration regions—have been elusive.

Multiple techniques have been used to measure particle fluxes over surfaces, including the use of wind tunnels in laboratory experiments (31), but micrometeorological techniques (32) have

recently emerged in the literature as preferred techniques. Pryor et al. (33) provide a rigorous analysis of these micrometeorological techniques, so we only briefly summarize them here.

The EC method is the most direct micrometeorological technique used for determining the vertical turbulent flux and exchange rate of particles over a given ecosystem (33). The EC technique measures surface–atmosphere exchange, or flux (F), by averaging the deviations from the mean of vertical wind speed (w') and concentration (c'), typically over 30 min (32, 34):

$$F = \langle w'c' \rangle. \quad 3.$$

Concentration may be taken as aerosol number or mass within a chosen size bin. This approach requires measurements of vertical wind speed (typically by a sonic anemometer) and particle concentration (typically by fast optical sensors either as a size-resolved value or as an integrated sum of particles within the inlet or instrument sampling range). EC requires fast data acquisition (typically >5 Hz) and the appropriate physical location for sampling. Historically, individual condensation particle counters with known size cuts (35) were used to calculate particle fluxes. More recently, the instrument requirements are often met with rapid optical measurement techniques, often home-built or modified commercial instrumentation (11), although some more recently available commercial analyzers are capable of size-resolved particle flux measurements (12, 36). Mass spectrometry–based instruments can provide chemical resolution but are typically unable to provide rapid size resolution (37, 38). The choice of sampling location must reflect several important assumptions. Measurements must be representative of an upwind area and be within the boundary layer of interest to ensure that the so-called fetch (i.e., the area over which measurements are being integrated) is adequate. The terrain must be horizontal and uniform, and the flux must be fully turbulent (i.e., most of the vertical transfer must be done by eddies). Meeting these requirements is challenging, as exemplified in studies over terrains with high roughness (39).

Alternate micrometeorological techniques for size-resolved particle fluxes include the relaxed eddy accumulation (REA) technique, which enables slower detection techniques by separately sampling drafts in the upward versus downward (and, ideally, neutral) directions (40). REA measurements of size-resolved particles have been successfully implemented over several forest sites (40, 41) and often provide comparable results to EC approaches (42). Held et al. (43, 44) also successfully deployed disjunct sampling techniques. For example, these researchers (44) applied single-particle, time-of-flight mass spectrometry to disjunct eddy sampling to derive chemically resolved particle fluxes; however, the required data processing was substantial.

The gradient approach is simpler still, with measurements at fixed heights along a vertical gradient coupled to sonic anemometers, thus enabling users to derive vertical fluxes. This approach makes many assumptions regarding turbulence conditions and requires comparable measurements at different heights. Aerosol particles have size-dependent losses in inlet lines and are subject to gas-particle partitioning, thus making gradient measurements with different inlet lengths (or bends in inlet lines if they are identical in length) particularly challenging.

An indirect approach to quantifying dry deposition to surfaces is to collect particles deposited to proxy surfaces. However, these types of approaches are limited in the ability of proxy surfaces to both physically and chemically represent true ecosystem surfaces, the potential for deposited particles to change form or evaporate after deposition, and the inability of analytical techniques to resolve whether observed compounds deposited on surfaces are truly deposited as particles rather than gases. Large monitoring networks have successfully established measurements of particle deposition of specific chemical components (e.g., NO_3^-, SO_4^{2-}, or NH_4^+), but these measurements do not typically separate deposited aerosol by size and thus do not provide size-resolved flux information.

Even when all the requirements for micrometeorological flux measurements are met, there are numerous challenges inherent in interpreting observed size-resolved particle fluxes. Model–measurement comparisons typically assume that the aerosol flux measurement is driven entirely by dry deposition. However, particle flux observations often include upward fluxes that are indicative of source terms from (*a*) in-canopy chemistry and secondary organic aerosol formation, (*b*) bioaerosol or other primary emission, (*c*) gas-particle partitioning along vertical thermal gradients, or (*d*) in-canopy particle nucleation (5, 45–49). A sink term from deposition must be isolated to properly evaluate deposition models. This idea that chemically induced fluxes affect observations of deposition for total aerosol has been validated by the observation that the chemical components of aerosols deposit at different rates (20, 37, 50). Black carbon (BC) may provide a useful test of size-resolved dry deposition parameterizations, as it is not subject to the chemical interferences inherent in total aerosol flux measurements. Aerosol number measurements include significant contributions from organic aerosols and other chemical components that are subject to gas-particle partitioning or oxidation chemistry, while BC does not undergo significant chemical change on the timescale of turbulent eddies (<15 min) and so should be unaffected by these otherwise confounding processes.

Humidity poses an additional challenge in interpreting observed size-resolved particle fluxes. Particles typically contain water in the ambient air, depending on their size, hygroscopicity, and the ambient relative humidity. Our fundamental understanding of the factors that control the turbulent motion or gravitational settling of particles in the atmosphere is that these factors are influenced by the actual size of the particles. Thus, when measuring the size-dependent particle flux (i.e., the correlation between particle number concentration and vertical wind speed), particle size may be easier to interpret when the particle is wet rather than dry. This nuance is counter to many aerosol measurement approaches, in which ambient particles are typically dried before sizing. Vertical gradients in temperature or concentration can similarly cause shifts in aerosol size distribution on the timescales of vertical exchange (50, 51).

3. OBSERVATIONS OF PARTICLE DEPOSITION

There are few recent measurements of aerosol flux, and thus V_{dep} observations, over vegetated surfaces. This lack of observations is primarily due to the challenges inherent in obtaining aerosol flux measurements. While there are reviews of particle flux and deposition measurements, it has been over a decade since a comprehensive report of all current measurements—for all types of ecosystems—has been attempted (5, 52), although we note the recent work of Saylor et al. (13), Petroff & Zhang (53), and Emerson et al. (14). In **Table 1**, we have compiled an extensive list of dry deposition particle measurements, including the studies that report deposition velocities, along with information about measurement size range, method, and location. The table is organized first by general land type, whether grassland, forest, water, or snow and ice, and then by date. A selection of these available data is plotted in **Figure 3** to provide a clear visual representation of gaps in our observations. Here, these observations are used to understand the major questions still facing the study of aerosol dry deposition. **Figure 3** highlights the lack of measurements over the cryosphere and that the bulk of size-resolved particle flux measurements have been collected in the accumulation mode.

Size is clearly a key controlling variable in particle dry deposition (14, 52, 54). Small particles are more strongly influenced by deposition processes driven by Brownian diffusion, while larger particles are more strongly influenced by interception, impaction, and gravitational settling (**Figure 2**). As a result of these competing processes, described in detail in Section 4, deposition velocity typically exhibits a minimum in the accumulation mode. This minimum occurs because

Table 1 Size-resolved particle flux observations, separated by land use type, method, size range, and typical deposition velocity

Land use type	Site location and details	Method	Size range (μm)	V_{dep} (cm/s)	Reference
Grassland	Grass and filter paper	Gradient	0.08–32	0.01–7.2	Chamberlain (104)
	Moss (*Hypnum cupressiforme*) and Italian rye grass	Wind tunnel experiment	0.5	0.024	Clough (105)
	Wood River refinery complex, Illinois, USA	Eddy covariance	0.05–0.1	0.6 ± 0.4	Wesely et al. (106)
	Grass	Gradient	0.05–1	0.525	Garland & Cox (107)
	Mount St. Bernard Abbey near Coalville, Leicestershire, England	Gradient	5–30	2.4–7.0	Dollard & Unsworth (108)
	Champaign, Illinois, USA	Eddy covariance	0.15–2.5	−0.05– −0.16	Katen & Hubbe (109)
	Champaign, Illinois, USA	Eddy covariance	∼0.1–1	0.22 ± 0.06	Wesely et al. (110)
	South Charleston, Ohio, USA	Eddy covariance	<1	0.4–0.8	Hicks et al. (111)
	Moorland with *Eriophorun* and *Juncus* species, Great Dun Fell, England	Gradient	5–31	0.5–8.9	Gallagher et al. (112)
	Moorland with *Eriophorun* and *Juncus* species, Great Dun Fell, England	Gradient	2–30	2.1–3.9	Fowler et al. (113)
	Sports fields at the University of Essex, Colchester, England	Gradient	0.1–2	0.10 ± 0.03	Allen et al. (114)
	Transitional lowland raised bog, *Sphagnum* species, Auchencorth Moss field site, southeast Scotland	Eddy covariance	0.1–3	0.007–1.2	Nemitz et al. (115)
	Field of rye grass, Shedd, Oregon, USA	Eddy covariance	0.52	0.16–0.44	Vong et al. (116)
	Alfalfa (*Medicago sativa*) field, Southern Great Plains site, Lamont, Oklahoma, USA	Eddy covariance	0.07–0.6	0.03 ± 0.02	Emerson et al. (68)
	Grass cuttings and synthetic commercial grass	Gradient	0.24–7.8	0.046–2.3	Connan et al. (117)
Forest	Solling forest (spruce and beech trees)	Gradient	0.26–2.4	0.7–1.8	Höfken & Gravenhorst (118)
	Königstein, Frankfurt, Germany	Gradient	0.1–10	1.4–1.9	Grosch & Schmitt (119)
	Spruce forest	Gradient	0.5–10	0.8–1.6	Waraghai & Gravenhorst (120)
	Pine plantation	Gradient	0.5–5	0.34–0.92	Lorenz & Murphy (121)
	Douglas fir forest, Speulderbos, The Netherlands	Eddy covariance	0.1–3	0.02–11	Gallagher et al. (122)
	Scots pine forest (SMEAR II station), Hyytiäälä, Finland	Eddy covariance	0.012–1	NA	Buzorius et al. (46)
	Scots pine forest (SMEAR II station), Hyytiäälä, Finland	REA	0.05	0.43 ± 0.06	Gaman et al. (40)
	Norway spruce forest (Waldstein research site), Germany	Eddy covariance	0.003–0.8	−0.23–0.37	Held et al. (123)

(*Continued*)

Table 1 (*Continued*)

Land use type	Site location and details	Method	Size range (μm)	V_{dep} (cm/s)	Reference
	Beech forest (CarboEuroFlux experimental forest site), Sorø, Denmark	Eddy covariance	0.02–0.07	0.15–0.45	Pryor (124)
	Scots pine forest (SMEAR II station), Hyytiäälä, Finland	REA	0.008–0.15	0.6–2.1	Grönholm et al. (56)
	Beech forest, Sorø, Denmark Scots pine forest (SMEAR II station), Hyytiälä, Finland	Eddy covariance and REA	0.01–0.1	0.2–0.5	Pryor et al. (33)
	Reserva Biológica do Cuieiras, Manaus, Brazil	Eddy covariance	0.01–0.1	NA	Ahlm et al. (103)
	Scots pine forest (SMEAR II station), Hyytiäälä, Finland	Eddy covariance	0.01–0.06	0.06–0.5	Grönholm et al. (125)
	Mixed deciduous forest: sugar maple, tulip poplar, sassafras, white oak, and black oak, Morgan-Monroe State Forest, Indiana, USA	Eddy covariance	0.008–0.1	0.06–0.3	Pryor et al. (10)
	Wet tropical rainforest, Amazonia, Brazil	Eddy covariance	0.25–2.5	NA	Ahlm et al. (36)
	Cuieiras, Manaus, Brazil	Eddy covariance	0.01–0.3	Reports flux	Rizzo et al. (35)
	Ponderosa pine plantation	Eddy covariance	0.25–1.0	0.2–0.6	Vong et al. (11)
	Mix of hardwood and coniferous trees, Borden Forest Research Station, Ontario, Canada	Eddy covariance	0.018–0.452	0.08–0.6	Gordon et al. (126)
	Scots pine forest (SMEAR II station), Hyytiäälä, Finland	Eddy covariance	0.01–0.3	0.07–0.4	Mammarella et al. (97)
	Aleppo pine trees (Yatir Forest Research Station), Israel	Eddy covariance	0.25–0.65	NA	Lavi et al. (39)
	Laboratory	Wind tunnel experiments	0.5–200	0.9–13	Zhang et al. (127)
	Norway spruce forest (Waldstein research site), Germany	Eddy covariance	0.006–1.4	−0.27	Deventer et al. (128)
	Temperate broadleaf forest, Ontario, Canada	Eddy covariance	0.05–0.5	NA	Petroff et al. (12)
Water	Laboratory	Wind tunnel experiments	0.04–1.5	0.01–0.04	Möller & Schumann (129)
	Laboratory	Wind tunnel experiments	0.3–28	0.004–38	Sehmel & Sutter (130)
	Laboratory	Wind tunnel experiments	0.1–1	NA	Larsen et al. (131)
	Southwest coast near Falkenberg, Sweden	Gradient	0.05–10	NA	Gustafsson & Franzén (132)
	Lake Michigan, USA	Gradient	0.25–100	0.06–5	Zufall et al. (133)

(*Continued*)

Table 1 (*Continued*)

Land use type	Site location and details	Method	Size range (μm)	V_{dep} (cm/s)	Reference
	Lake Michigan, USA	Physical sampling	0.05–50	0.004–11	Caffrey et al. (134)
	Baltic Sea	Gradient	1–20	Only reports flux	Petelski (135)
	Surf zone on the island of Østergarnsholm, Sweden	Physical sampling	0.5–20	NA	Pryor et al. (136)
	Northwest Pacific Ocean: Yellow Sea and East China Sea	Physical sampling	~0.5–35	NA	Zhang et al. (137)
	Yellow Sea	Physical sampling	~0.5–11	NA	Shi et al. (138)
	Laboratory	Wind tunnel experiments	~0.18	6×10^{-5}–0.004	Calec et al. (139)
	Marginal seas of China (Yellow Sea, Bohai Sea, East China Sea, and South China Sea) and the Northwest Pacific Ocean	Physical sampling	~0.5–11	0.0052–6.97	Qi et al. (140)
Snow and ice	Snow field	Physical sampling	0.7–7	0.035–0.14	Ibrahim et al. (88)
	Snow-covered field (Pennsylvania State University Agricultural Research Farm), Rock Springs, PA	Eddy covariance	0.15–1	0.021–0.034	Duan et al. (87)
	Snow-covered Sitka spruce forest, Dunslair Heights, Scotland	Eddy covariance	3–31	−4.4–50.9	Gallagher et al. (91)
	Arctic Ocean ice floe	Eddy covariance	0.01–1	0.05–0.14	Nilsson & Rannik (89)
	Smooth snow surface, Dronning Maud Land, Antarctica	Eddy covariance	0.01–0.85	0.08–1.89	Grönlund et al. (90)
	Iced branch of the Ross Sea, Nansen Ice Sheet, Antarctica	Eddy covariance	0.01–1	0.06 ± 0.09	Contini et al. (86)
	Neil Trivett Global Atmosphere Watch Observatory Alert, Nunavut, Canada	Physical sampling	0.07–0.5	0.03 ± 0.09	Macdonald et al. (92)

This table excludes urban fluxes (see Section 6.3).
Abbreviations: NA, not available; REA, relaxed eddy accumulation.

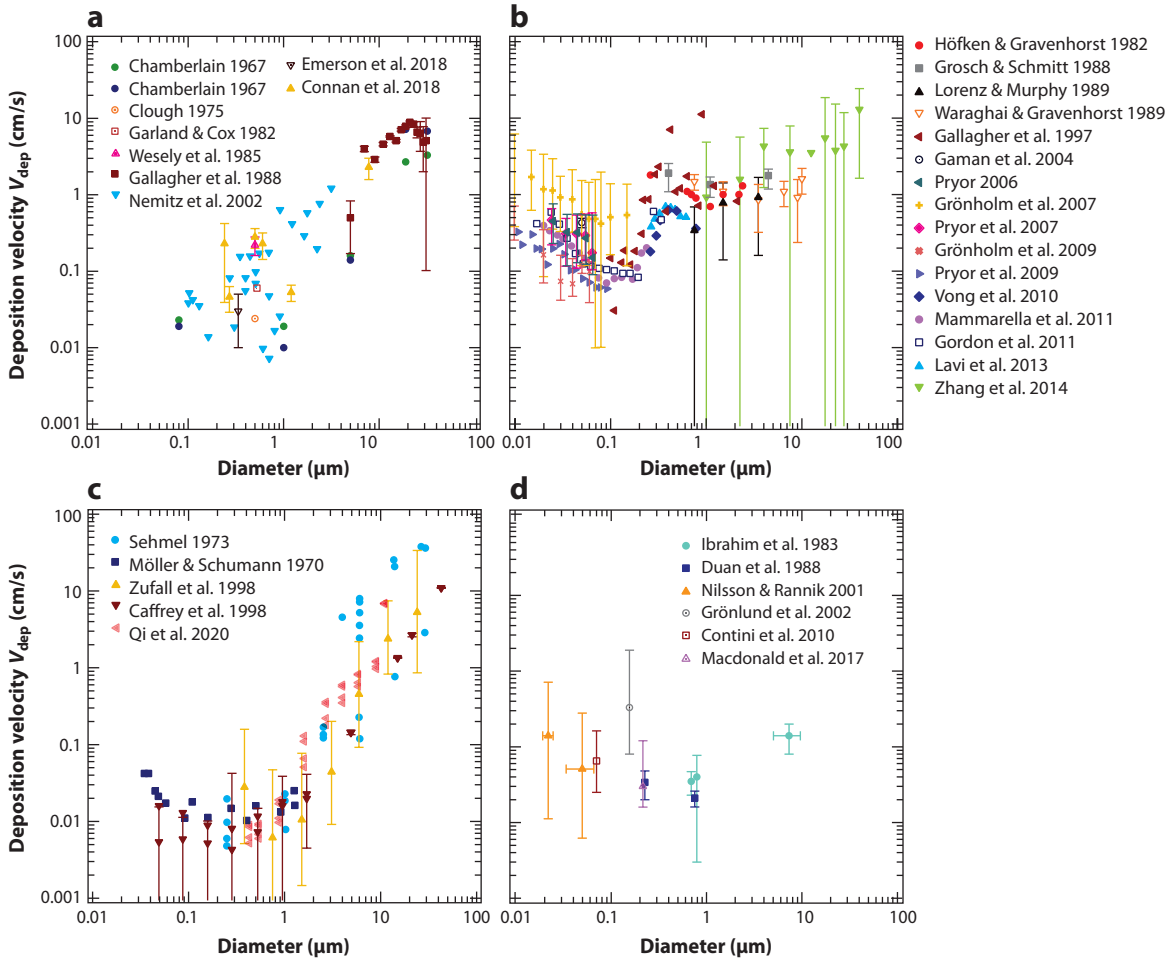

Figure 3

Graphs showing compiled multiple size–resolved particle flux observations of deposition velocity as a function of size over (*a*) grasslands, (*b*) forests, (*c*) water surfaces, and (*d*) the cryosphere. These data sets are not normalized for friction velocity (u^*), which has been established to strongly influence flux.

uptake to surface collectors due to Brownian diffusion decreases as size increases, while removal by gravitational settling increases with size. The roles of surface uptake due to impaction and interception processes also increase with size, though models suggest a drop-off at the very large (i.e., tens of microns in diameter) size range. Of course, the relevance of different aerosol modes or size ranges depends on the question being posed; small particles are typically greater in number but can be less important in terms of mass exchange.

Deposition velocities are clearly a function of turbulence (typically described by friction velocity, u^*), with more turbulent conditions inducing a stronger flux (11, 36, 55, 56). Land use type also impacts deposition velocity, with more complex ecosystems with greater surface area holding more collectors and enabling more deposition through interception. Hence, deposition velocities over forests are typically greater than those over grasslands, which are in turn greater than those over lakes or smooth aquatic surfaces. At larger particle sizes (>10 μm in diameter), gravitational

settling plays a controlling role, and deposition rates tend to converge independent of surface structure.

4. CURRENT MODELS AND OUR MECHANISTIC UNDERSTANDING

One major challenge in modeling aerosol concentrations is the prediction of deposition trends over a wide range of land use types, while maintaining the ability of the model to be assimilated easily into global transport and climate models. Models typically use an aerosol deposition module with a particle size–dependent resistance approach tailored for terrestrial surfaces (7, 57). Slinn (16) developed a resistance approach to model deposition to various vegetative canopies using land use–specific resistances. The parameterization developed by Zhang et al. (19) expanded on the Slinn approach by incorporating simple empirical parameterizations for dry deposition processes. Zhang et al. (19) also expanded the application of the resistance approach to 14 different land use types, including water and ice surfaces.

The Zhang et al. framework is currently used in multiple chemical transport and climate models [including GLOMAP (Global Model of Aerosol Processes) and GEOS-Chem]. Both Slinn (16) and Zhang et al. (19) describe the particle size–dependent deposition velocity (V_{dep}) as

$$V_{dep} = V_g + \frac{1}{R_a + R_s}, \quad 4.$$

where V_g is the gravitational settling speed, which is a function of particle density, diameter, the viscosity of air, and a correction factor for small particles derived from the mean free path of molecules in air, temperature, pressure, and kinematic viscosity. R_a and R_s are the aerodynamic and quasilaminar sublayer resistances, respectively,

$$R_a = \frac{\ln(z_r, z_o) - \Psi_H}{\kappa u^*}, \quad 5.$$

$$R_s = \frac{1}{\varepsilon_o u^* (E_B + E_{IN} + E_{IM}) R_i}, \quad 6.$$

where z_r is the height, z_o is the roughness length, Ψ_H is the stability function, κ is the von Karman constant, and u^* is the friction velocity. In the quasilaminar sublayer equation, ε_o is an empirical constant, R_i represents the fraction of particles stuck to a surface, and E_B, E_{IN}, and E_{IM} are the collection efficiencies of Brownian diffusion, interception, and impaction, respectively. Zhang et al. (19) take E_B and E_{IN} from Slinn (16) and E_{IM} from Peters & Eiden (58),

$$E_B = Sc^{-\gamma}, \quad 7.$$

$$E_{IN} = \frac{1}{2}\left(\frac{D_p}{A}\right)^2, \quad 8.$$

$$E_{IM} = \left(\frac{St}{\alpha + St}\right)^{\beta}, \quad 9.$$

where Sc is the Schmidt number and St is the Stokes number (calculated from the gravitational deposition velocity, the friction velocity, and either the kinematic viscosity of air for oceans and other smooth surfaces or the acceleration due to gravity and a characteristic radius that depends on the collection surface A). The other four variables represented in these equations are land use–dependent constants for the collection efficiencies: γ (Brownian diffusion), A (interception),

α (impaction), and β (impaction). Zhang et al. (19) tuned the γ, A, α, and roughness length (z_o) variables for each of the 14 land use types employed in the model. The β term was taken to equal a value of 2 for all land use types by Zhang et al. (19).

Slightly different frameworks for describing aerosol dry deposition also exist (e.g., 59) but are not commonly used in atmospheric chemical transport models. Alternate equations for the collection efficiency of interception (EIN) and the efficiency of impaction (EIM) have been proposed by Slinn (16), Giorgi (60, 61), Pleim & Ran (62), Petroff & Zhang (53), and Emerson et al. (14) but are infrequently incorporated into global models. These alternate parameterizations are rarely evaluated against aerosol observations. In a key piece of work, Saylor et al. (13) implemented several of these deposition algorithms in a regional air quality model and found that fine particle concentrations varied from 5 to 15% depending on the deposition algorithm, with total deposition varying by over 200%. Emerson et al. (14) revised the Zhang et al. parameterization constrained by observations in a chemical transport model and noted that global surface accumulation mode number concentrations increased by 62% compared to those in the Zhang et al. parameterization and thus impacted the aerosol direct and indirect effects substantially. A closer investigation of these algorithms and model–measurement comparison was clearly warranted.

While the values described by Zhang et al. (19) have been compared to some observations over vegetated surfaces, the parameters used to tune modern deposition models to ocean surfaces have not been tested against observations. This is likely due to the lack of aerosol flux observations, in particular size-resolved aerosol flux measurements, over the ocean, and the fact that these observations include both a source term from sea spray and a sink term from deposition that must be separated to properly evaluate the deposition model. Aerosol dry deposition models that are specific for ocean and water surfaces endeavor to address wind speed dependence and processes specific to the marine environment (e.g., 63–67). However, these models are infrequently used in global models.

A more recent model developed by Petroff & Zhang (53) was better able to capture deposition trends over 26 different defined land use types. The Petroff & Zhang parameterizations are more sensitive to surface changes because of the revised form of the deposition velocity that considers the leaf area index as well as canopy height. The model also includes the ground below the canopy as a surface for deposition. The second major difference between Petroff & Zhang (53) and Zhang et al. (19) is the parameterization of Brownian diffusion, interception, and inertial impaction as well as the inclusion of turbulent impaction by Petroff & Zhang (53):

$$E_{\mathrm{IB}} = C_{\mathrm{B}} Sc^{\frac{-2}{3}} Re^{-\frac{1}{2}}, \tag{10.}$$

$$E_{\mathrm{IN}} = C_{\mathrm{IN}} \left(\frac{\mathrm{d}p}{A}\right) \text{ (needlelike obstacles)}, \tag{11a.}$$

$$E_{\mathrm{IN}} = C_{\mathrm{IN}} \left(\frac{\mathrm{d}p}{A}\right) \left[2 + \ln\left(\frac{4A}{\mathrm{d}p}\right)\right] \text{ (leaf or plane obstacles)}, \tag{11b.}$$

$$E_{\mathrm{IM}} = C_{\mathrm{IM}} \left[\frac{St}{(\alpha + St)}\right]^{\beta}, \tag{12.}$$

$$E_{\mathrm{IT}} = \left(2.5 \times 10^{-3}\right) \times C_{\mathrm{IT}} \times \left(\tau_{\mathrm{ph}}\right)^2 \text{ if } \tau_{\mathrm{ph}} < 20, \tag{13a.}$$

$$E_{\mathrm{IT}} = C_{\mathrm{IT}} \text{ if } \tau_{\mathrm{ph}} \geq 20, \tag{13b.}$$

where Re is the Reynolds number on top of the canopy and C_{B}, C_{IN}, C_{IM}, and C_{IT} are numerical coefficients for Brownian diffusion, interception, inertial impaction, and turbulent impaction,

respectively. These constants are adjusted based on the land use type. In Equation 13, τ_{ph} represents the nondimensional particle relaxation time. The interception deposition efficiency (Equation 11) has two forms, the first for needlelike obstacles and the second for leaf or plane obstacles. The β term was also taken to equal a value of 2 for all land use types, just as it was by Zhang et al. (19).

Another important improvement in the work of Petroff & Zhang (53) was the incorporation of velocity attributed to the phoretic effects (V_{phor}) observed over water, ice, and snow surfaces into the calculation of the drift velocity. This addition significantly increased the accuracy of the predicted size-resolved deposition over these surfaces. When compared to observed deposition measurements for water surfaces, Petroff & Zhang (68) were able to accurately capture the minimum in the deposition trend using the V_{phor} term. For snow and ice surfaces, the improvement is less obvious due to the scarce number of direct deposition measurements over those surfaces to compare with the model.

While the Petroff & Zhang (53) parameterization compares better with observations, it is not currently used in global transport and climate models. One reason for this may be that Petroff & Zhang (53) defined a total of 26 land use categories compared to the 14 originally incorporated into global models. Changing these fundamental parameterizations may have made the Petroff & Zhang algorithm more difficult to assimilate into current deposition modules than is the frequently used Zhang (19) parameterization. Emerson et al. (14) aimed to strike a balance between these challenges by maintaining the structure of the key Zhang parameterization while capturing observed size dependence in dry deposition. While a robust parameterization that agrees well with the available direct deposition measurements is clearly needed in global models, the framework needs to be constrained enough to be easily incorporated into a broad array of chemical transport models and existing deposition modules.

5. BLACK CARBON

BC is a particularly important material for understanding aerosol lifetime: It is chemically stable and nonvolatile, is only formed in combustion, and can be sensitively and selectively detected both in the air and in the cryosphere postdeposition. When deposited on snow surfaces, BC increases the absorption of sunlight by the surface, enhancing snow aging and melting (69) and generating positive climate feedback (70).

BC directly impacts atmospheric temperature via the absorption of solar radiation and indirectly impacts cloud formation and the optical properties of clouds (71). Upon deposition to snow and ice surfaces, BC can alter surface albedo and enhance snowmelt (70, 72). Key BC sources include the combustion of fossil fuels and biofuels as well as biomass burning and wildfires (73). Major sinks are both dry and wet deposition through scavenging by cloud droplets, ice crystals, and precipitation. While much recent work has focused on the sources, aging, and optical properties of BC (e.g., see 73, and references therein), the deposition component of the BC life cycle remains poorly constrained.

BC deposition to snow and ice surfaces links anthropogenic pollution, changes in the planet's radiative balance, and human impacts. Recent work (e.g., 74–77) has linked BC deposition on snowpacks to more rapid snowmelt and thus the water supply for agriculture and population centers in the Himalayas, the Cascade Range, and the Sierra Nevada of California. Hadley et al. (74) noted that atmospheric BC concentrations decreased during snowfall events, suggesting that the bulk of BC that was deposited to the Sierra Nevada snowpack was the result of scavenging below clouds rather than ice nucleation. The authors also noted that BC in the Sierra Nevada snowfall would darken the fresh snow to such an extent that its albedo could be reduced by >1% (74). In contrast, Yasunari et al. (77) found that dry deposition in the premonsoon season of the

Himalayas was particularly important for albedo reduction of mountain glaciers and thus the timing of snowmelt. However, predictions of BC concentrations in snow and their consequent effects on albedo, surface temperatures, and snowmelt rely on accurate representations of the wet and dry deposition of BC as well as on the evolution of snow on seasonal timescales (e.g., snow metamorphism, sublimation, melt, and blowing). Yasunari et al. (77, p. 266) noted that "how to estimate [BC dry deposition velocity] more accurately at the grid point, which includes snowcover or glacier surface, is the key to assessing glacier retreats or seasonal snow melt timings, in terms of the debris-covered area, snow darkening effect due to climate and environmental changes, using climate models." Other work has suggested that wet deposition and transport dominate the lifetime of BC in the Arctic (78), and that more observational constraints on wet deposition in particular are essential. The uncertainties in accurately predicting BC in or on snow surfaces, and thus its effects on albedo and snowmelt, are directly linked to the poor understanding of deposition and the lack of BC deposition measurements.

The single-particle soot photometer (79, 80) offers an intriguing opportunity to make EC surface–atmosphere flux measurements of refractory BC. Emerson et al. (68) demonstrated that this instrument can be coupled to the EC approach to provide direct flux observations of BC over a grassland, while Joshi et al. (81) demonstrated its flux measurement capacity over the far more polluted urban environment of Beijing.

6. OPEN QUESTIONS

Our understanding of the dry deposition of size-dependent particles is poor due to the lack of field observations. To reduce model uncertainty, we require a deeper understanding of size-dependent particle dry deposition rates over key terrestrial and aquatic surfaces. Water surfaces and the cryosphere are two particularly poorly understood surfaces for particle dry deposition.

6.1. Water Surfaces

Clouds in the marine boundary layer have a particularly strong but poorly constrained influence on climate (82, 83). Clouds are most susceptible to changes due to aerosols when clouds have low optical depth, large horizontal extent, and low aerosol concentrations, as in, for example, the stratocumulus regions of the subtropical oceans (84, 85). Uncertainties in size-dependent aerosol dry deposition rates dominate CCN prediction uncertainties over remote global ocean regions, particularly in regions with low precipitation rates (4). Uncertainties in remote ocean CCN mean that uncertainties in dry deposition could be the leading contributor to uncertainties in aerosol indirect effects globally due to high cloud susceptibility in many remote ocean regions (2). These results strongly emphasize the need for increased certainty about dry deposition rates over oceans in models (2, 4).

6.2. The Cryosphere

Surface properties clearly influence deposition, and while we have developed appropriate parameterizations for dry deposition in forest and grassland ecosystems, we expect the cryosphere to behave as a very different surface for particle uptake due to its distinct chemical and physical properties relative to leaf surfaces.

Direct measurements of dry deposition over ice- and snow-covered surfaces are limited (86–89). Deposition velocities over rough surfaces have been shown to be considerably higher (>100%) than those reported over smooth snow-covered surfaces (90). Gallagher et al. (91) observed a similar phenomenon in which the introduction of snowfall to a spruce forest resulted in

a twofold reduction in the flux of cloud droplets to the canopy. However, the characteristic size-resolved trend is still present in the data, with ultrafine (<0.1 μm in diameter) and coarse mode (typically 2.5–10 μm in diameter) particles depositing faster than do accumulation mode particles. Seasonal differences in deposition have also been observed in the cryosphere. Macdonald et al. (92) showed that deposition for accumulation mode BC increased during warmer months. This trend is thought to be a result of increased scavenging by mixed-phase clouds during those periods. Measurements with higher size resolution over longer periods are needed to fully understand how these surfaces change particle deposition in the cryosphere.

Accurately characterizing BC dry deposition is particularly important for regions with large amounts of snow and ice cover because of the high impact of BC on surface albedo. Huang et al. (93) showed that the alteration of dry deposition parameterizations over the base model was essential for correctly modeling surface BC concentrations in the Arctic; the use of an unaltered dry deposition module caused the underestimation of surface BC by factors of at least two and often five or more. Huang et al. (93) used the size-resolved resistance-in series approach of Zhang et al. (19). However, to the best of our knowledge, this dry deposition parameterization has never been tested against BC deposition, only total (refractory plus nonrefractory) aerosol deposition. An assessment of current deposition models against an observational data set of aerosol fluxes over the cryosphere is clearly needed.

6.3. Phoretic Effects

For water, snow, and ice surfaces in comparison to vegetative surfaces, additional factors impact particle deposition. Near-surface gradients in temperature, water vapor, and electricity all have the potential to alter the movement of particles toward the collecting surfaces. These surface effects are collectively referred to as phoretic effects. Both thermophoresis, which is caused by temperature gradients, and diffusiophoresis, which is caused by gradients in water vapor concentration, are speculated to impact the deposition of fine particles. While these phoretic effects can force particle movement toward cold and evaporating surfaces, the Stefan flow effect induces particle flow toward a condensing surface. The impact of electrophoresis on particle deposition is not well constrained. Tammet et al. (94) investigated these effects through a model study and found them to be essential mechanisms for the deposition of 10–200-nm particles during periods of low wind speed; however, strong wind speeds appear to suppress this mechanism. The full characterization of these effects requires targeted near-surface measurements of the magnitude of these gradients.

6.4. Other Terrestrial Surfaces

Earth's terrestrial surface is diverse, with different plant structures that induce different turbulent dependencies and collection efficiencies and thus different deposition rates. Furthermore, plant morphology and physiology are not static; these factors change as ecological succession progresses and with seasonal cycles. The role of these changes in surface structure is poorly understood but may have substantive effects on aerosol dry deposition and thus atmospheric lifetime. For example, Pryor et al. (95) observed enhanced deposition rates for ultrafine (<100 nm in diameter) particles over a midwestern US forest during leaf-out relative to bare trees and were able to attribute the bulk of ultrafine particle deposition to canopy uptake (rather than to the ground). In contrast, Rannik et al. (96) investigated long-term integrated (i.e., not size-segregated) fluxes over a boreal pine forest and found stronger particle deposition fluxes in the winter than in the summer; however, the researchers attributed this seasonal variability to shifts in size distribution rather than to surface collectors (97).

Urban surfaces are a particularly challenging type of region to study, as airflows and micrometeorology in urban environments are complex. EC measurements are challenging and rarely done, although several recent studies have successfully characterized urban emissions of particles from vehicle exhaust and other sources (47, 98–102). Deriving the deposition term over urban surfaces is more challenging, as it requires measurements far downwind of major sources or a strong understanding of the simultaneous emissions. However, it is intriguing that several of these studies have been able to observe deposition over urban parks (101, 102).

7. CONCLUSIONS

With the exception of urban, ocean, and chemically resolved particle flux studies, most work to date assumes that observed downward fluxes represent purely depositional processes. However, upward fluxes are frequently observed, whether over forests or grasslands (45, 95, 103). While such observations are reasonable over urban or marine areas where primary emission sources may be substantial, upward fluxes over remote regions have proven to be more puzzling and have often been attributed to particle nucleation, entrainment, or vertical gradients in gas-particle partitioning. However, Emerson et al.'s recent observation (68) of upward BC fluxes over a grassland site suggests that upward fluxes may be ubiquitous and that contributing processes such as resuspension warrant further investigation.

The dry deposition of particles is an underappreciated uncertainty in our ability to predict both the radiative and health effects of atmospheric aerosols. However, newer instruments developed over the past 20 years have enabled an array of new field observations of size-resolved particle fluxes. Beyond size resolution, the addition of chemical resolution in particle flux measurements would be particularly useful for separating the different driving mechanisms responsible for upward and downward fluxes. For example, our 2017 measurements (68) of BC wet deposition and surface–atmosphere exchange fluxes over a southern Great Plains site in Oklahoma allowed us to quantify the relative importance of wet versus dry deposition. In that study, we observed that wet deposition dominated dry deposition at the site during the campaign, resulting in dry deposition accounting for about 6% of the loss and a net lifetime for BC of 7 to 11 days. However, these observations were limited to one location over just a few weeks, and many more measurements over many different environments are essential for more generally constraining the importance of and the mechanisms behind particle dry deposition.

While measurements over terrestrial ecosystems have increased in number over the past 20 years, Earth's surface is complex. Fundamentally improving our understanding of deposition—and thus our capacity to model it—requires additional observations over the cryosphere, water surfaces, urban systems, and the biosphere.

DISCLOSURE STATEMENT

The authors are not aware of any affiliations, memberships, funding, or financial holdings that might be perceived as affecting the objectivity of this review.

ACKNOWLEDGMENTS

This work was supported by the National Oceanic and Atmospheric Administration Climate Program Office's Atmospheric Chemistry, Carbon Cycle, and Climate program (grant NA14OAR4310141) and the Department of Energy Office of Biological and Environmental Research (grant DE-SC0016259).

LITERATURE CITED

1. IPCC (Intergov. Panel Clim. Chang.). 2013. *Climate Change 2013: The Physical Science Basis. Contribution of Working Group I to the Fifth Assessment Report of the Intergovernmental Panel on Climate Change*. Cambridge, UK/New York: Cambridge Univ. Press
2. Carslaw KS, Lee LA, Reddington CL, Pringle K, Rap A, et al. 2013. Large contribution of natural aerosols to uncertainty in indirect forcing. *Nature* 503:67–71
3. Lee LA, Carslaw KS, Pringle KJ, Mann GW. 2012. Mapping the uncertainty in global CCN using emulation. *Atmos. Chem. Phys.* 12:9739–51
4. Lee LA, Pringle KJ, Reddington CL, Mann GW, Stier P, et al. 2013. The magnitude and causes of uncertainty in global model simulations of cloud condensation nuclei. *Atmos. Chem. Phys.* 13:8879–914
5. Pryor SC, Gallagher M, Sievering H, Larsen SE, Barthelmie RJ, et al. 2008. A review of measurement and modelling results of particle atmosphere–surface exchange. *Tellus B Chem. Phys. Meteorol.* 60:42–75
6. Fowler D, Pilegaard K, Sutton MA, Ambus P, Raivonen M, et al. 2009. Atmospheric composition change: ecosystems–atmosphere interactions. *Atmos. Environ.* 43:5193–267
7. Wesely ML, Hicks BB. 2000. A review of the current status of knowledge on dry deposition. *Atmos. Environ.* 34:2261–82
8. Ruijrok W, Davidson CI, Nicholson KW. 1995. Dry deposition of particles. *Tellus B Chem. Phys. Meteorol.* 47:587–601
9. Pryor SC, Barthelmie RJ, Hornsby KE. 2013. Size-resolved particle fluxes and vertical gradients over and in a sparse pine forest. *Aerosol Sci. Technol.* 47:1248–57
10. Pryor SC, Barthelmie RJ, Spaulding AM, Larsen SE, Petroff A. 2009. Size-resolved fluxes of sub-100-nm particles over forests. *J. Geophys. Res. Atmos.* 114:D18212
11. Vong RJ, Vong IJ, Vickers D, Covert DS. 2010. Size-dependent aerosol deposition velocities during BEARPEX'07. *Atmos. Chem. Phys.* 10:5749–58
12. Petroff A, Murphy J, Thomas S, Geddes J. 2018. Size-resolved aerosol fluxes above a temperate broadleaf forest. *Atmos. Environ.* 190:359–75
13. Saylor RD, Baker BD, Lee P, Tong D, Pan L, Hicks BB. 2019. The particle dry deposition component of total deposition from air quality models: right, wrong or uncertain? *Tellus B Chem. Phys. Meteorol.* 71:1550324
14. Emerson EW, Hodshire AL, DeBolt HM, Bilsback KR, Pierce JR, et al. 2020. Revisiting particle dry deposition and its role in radiative effect estimates. *PNAS* 117:26076–82
15. Goldstein AH, Galbally IE. 2007. Known and unexplored organic constituents in the Earth's atmosphere. *Environ. Sci. Technol.* 41:1514–21
16. Slinn WGN. 1982. Predictions for particle deposition to vegetative canopies. *Atmos. Environ.* 16:1785–94
17. Farmer DK, Cappa CD, Kreidenweis SM. 2015. Atmospheric processes and their controlling influence on cloud condensation nuclei activity. *Chem. Rev.* 115:4199–217
18. Pöschl U. 2005. Atmospheric aerosols: composition, transformation, climate and health effects. *Angew. Chem. Int. Ed.* 44:7520–40
19. Zhang LM, Gong SL, Padro J, Barrie L. 2001. A size-segregated particle dry deposition scheme for an atmospheric aerosol module. *Atmos. Environ.* 35:549–60
20. Ruijgrok W, Tieben H, Eisinga P. 1997. The dry deposition of particles to a forest canopy: a comparison of model and experimental results. *Atmos. Environ.* 31:399–415
21. Stevens CJ, Dise NB, Mountford JO, Gowing DJ. 2004. Impact of nitrogen deposition on the species richness of grasslands. *Science* 303:1876–79
22. Fowler D, Coyle M, Skiba U, Sutton MA, Cape JN, et al. 2013. The global nitrogen cycle in the twenty-first century. *Philos. Trans. R. Soc. B Biol. Sci.* 368:20130164
23. Schiferl LD, Heald CL, Kelly D. 2018. Resource and physiological constraints on global crop production enhancements from atmospheric particulate matter and nitrogen deposition. *Biogeosciences* 15:4301–15
24. Erisman JW, Draaijers G, Duyzer J, Hofschreuder P, Van Leeuwen N, et al. 1997. Particle deposition to forests—summary of results and application. *Atmos. Environ.* 31:321–32

25. Vicars WC, Sickman JO, Ziemann PJ. 2010. Atmospheric phosphorus deposition at a montane site: size distribution, effects of wildfire, and ecological implications. *Atmos. Environ.* 44:2813–21
26. Bobbink R, Hicks K, Galloway J, Spranger T, Alkemade R, et al. 2010. Global assessment of nitrogen deposition effects on terrestrial plant diversity: a synthesis. *Ecol. Appl.* 20:30–59
27. Casal P, Zhang Y, Martin JW, Pizarro M, Jiménez B, Dachs J. 2017. Role of snow deposition of perfluoroalkylated substances at coastal Livingston Island (maritime Antarctica). *Environ. Sci. Technol.* 51:8460–70
28. Hageman KJ, Hafner WD, Campbell DH, Jaffe DA, Landers DH, Simonich SLM. 2010. Variability in pesticide deposition and source contributions to snowpack in western US national parks. *Environ. Sci. Technol.* 44:4452–58
29. Rose NL, Rippey B. 2002. The historical record of PAH, PCB, trace metal and fly-ash particle deposition at a remote lake in north-west Scotland. *Environ. Pollut.* 117:121–32
30. McMurry PH. 2000. A review of atmospheric aerosol measurements. *Atmos. Environ.* 34:1959–99
31. Zufall MJ, Dai WP, Davidson CI. 1999. Dry deposition of particles to wave surfaces: II. Wind tunnel experiments. *Atmos. Environ.* 33:4283–90
32. Baldocchi DD, Hicks BB, Meyers TP. 1988. Measuring biosphere-atmosphere exchanges of biologically related gases with micrometeorological methods. *Ecology* 69:1331–40
33. Pryor S, Larsen SE, Sørensen LL, Barthelmie RJ, Grönholm T, et al. 2007. Particle fluxes over forests: analyses of flux methods and functional dependencies. *J. Geophys. Res. Atmos.* 112:D07205
34. Baldocchi DD. 2003. Assessing the eddy covariance technique for evaluating carbon dioxide exchange rates of ecosystems: past, present and future. *Glob. Chang. Biol.* 9:479–92
35. Rizzo LV, Artaxo P, Karl T, Guenther AB, Greenberg J. 2010. Aerosol properties, in-canopy gradients, turbulent fluxes and VOC concentrations at a pristine forest site in Amazonia. *Atmos. Environ.* 44:503–11
36. Ahlm L, Krejci R, Nilsson ED, Martensson EM, Vogt M, Artaxo P. 2010. Emission and dry deposition of accumulation mode particles in the Amazon Basin. *Atmos. Chem. Phys.* 10:10237–53
37. Farmer DK, Kimmel JR, Phillips G, Docherty KS, Worsnop DR, et al. 2011. Eddy covariance measurements with high-resolution time-of-flight aerosol mass spectrometry: a new approach to chemically resolved aerosol fluxes. *Atmos. Meas. Tech.* 4:1275–89
38. Nemitz E, Jimenez JL, Huffman JA, Ulbrich IM, Canagaratna MR, et al. 2008. An eddy-covariance system for the measurement of surface/atmosphere exchange fluxes of submicron aerosol chemical species—first application above an urban area. *Aerosol Sci. Technol.* 42:636–57
39. Lavi A, Farmer DK, Segre E, Moise T, Rotenberg E, et al. 2013. Fluxes of fine particles over a semi-arid pine forest: possible effects of a complex terrain. *Aerosol Sci. Technol.* 47:906–15
40. Gaman A, Rannik Ü, Aalto P, Pohja T, Siivola E, et al. 2004. Relaxed eddy accumulation system for size-resolved aerosol particle flux measurements. *J. Atmos. Ocean. Technol.* 21:933–43
41. Schery SD, Wasiolek PT, Nemetz BM, Yarger FD, Whittlestone S. 1998. Relaxed eddy accumulator for flux measurement of nanometer-size particles. *Aerosol Sci. Technol.* 28:159–72
42. Pryor SC, Larsen SE, Sørensen LL, Barthelmie RJ. 2008. Particle fluxes above forests: observations, methodological considerations and method comparisons. *Environ. Pollut.* 152:667–78
43. Held A, Niessner R, Bosveld F, Wrzesinsky T, Klemm O. 2007. Evaluation and application of an electrical low pressure impactor in disjunct eddy covariance aerosol flux measurements. *Aerosol Sci. Technol.* 41:510–19
44. Held A, Hinz K-P, Trimborn A, Spengler B, Klemm O. 2003. Towards direct measurement of turbulent vertical fluxes of compounds in atmospheric aerosol particles. *Geophys. Res. Lett.* 30:2016
45. Pryor S, Barthelmie RJ, Sørensen LL, Larsen SE, Sempreviva AM, et al. 2008. Upward fluxes of particles over forests: when, where, why? *Tellus B Chem. Phys. Meteorol.* 60:372–80
46. Buzorius G, Rannik U, Makela JM, Vesala T, Kulmala M. 1998. Vertical aerosol particle fluxes measured by eddy covariance technique using condensational particle counter. *J. Aerosol Sci.* 29:157–71
47. Märtensson EM, Nilsson ED, Buzorius G, Johansson C. 2006. Eddy covariance measurements and parameterisation of traffic related particle emissions in an urban environment. *Atmos. Chem. Phys.* 6:769–85
48. Nemitz E, Sutton MA. 2004. Gas-particle interactions above a Dutch heathland: III. Modelling the influence of the NH_3-HNO_3-NH_4NO_3 equilibrium on size-segregated particle fluxes. *Atmos. Chem. Phys.* 4:1025–45

49. Trebs I, Lara LL, Zeri LMM, Gatti LV, Artaxo P, et al. 2006. Dry and wet deposition of inorganic nitrogen compounds to a tropical pasture site (Rondonia, Brazil). *Atmos. Chem. Phys.* 6:447–69
50. Farmer DK, Chen Q, Kimmel JR, Docherty KS, Nemitz E, et al. 2013. Chemically resolved particle fluxes over tropical and temperate forests. *Aerosol Sci. Technol.* 47:818–30
51. Pryor SC, Binkowski FS. 2004. An analysis of the time scales associated with aerosol processes during dry deposition. *Aerosol Sci. Technol.* 38:1091–98
52. Petroff A, Mailliat A, Amielh M, Anselmet F. 2008. Aerosol dry deposition on vegetative canopies. Part I: Review of present knowledge. *Atmos. Environ.* 42:3625–53
53. Petroff A, Zhang L. 2010. Development and validation of a size-resolved particle dry deposition scheme for application in aerosol transport models. *Geosci. Model Dev.* 3:753–69
54. Petroff A, Mailliat A, Amielh M, Anselmet F. 2008. Aerosol dry deposition on vegetative canopies. Part II: A new modelling approach and applications. *Atmos. Environ.* 42:3654–83
55. Sievering H. 1987. Small-particle dry deposition under high wind speed conditions: eddy flux measurements at the Boulder atmospheric observatory. *Atmos. Environ.* 1967 21:2179–85
56. Grönholm T, Aalto PP, Hiltunen VJ, Rannik Ü, Rinne J, et al. 2007. Measurements of aerosol particle dry deposition velocity using the relaxed eddy accumulation technique. *Tellus B Chem. Phys. Meteorol.* 59:381–86
57. Wesely ML. 1989. Parameterization of surface resistances to gaseous dry deposition in regional-scale numerical models. *Atmos. Environ.* 23:1293–304
58. Peters K, Eiden R. 1992. Modeling the dry deposition velocity of aerosol particles to a spruce forest. *Atmos. Environ. A* 26:2555–64
59. Giardina M, Buffa P. 2018. A new approach for modeling dry deposition velocity of particles. *Atmos. Environ.* 180:11–22
60. Giorgi F. 1986. A particle dry-deposition parameterization scheme for use in tracer transport models. *J. Geophys. Res. Atmos.* 91:9794–806
61. Giorgi F. 1988. Dry deposition velocities of atmospheric aerosols as inferred by applying a particle dry deposition parameterization to a general circulation model. *Tellus B Chem. Phys. Meteorol.* 40B:23–41
62. Pleim J, Ran L. 2011. Surface flux modeling for air quality applications. *Atmosphere* 2:271–302
63. Fairall CW, Hare JE, Edson JB, McGillis W. 2000. Parameterization and micrometeorological measurement of air–sea gas transfer. *Bound. Layer Meteorol.* 96:63–106
64. Sievering H. 1984. Small-particle dry deposition on natural waters: modeling uncertainty. *J. Geophys. Res. Atmos.* 89:9679–81
65. Slinn SA, Slinn WGN. 1980. Predictions for particle deposition on natural waters. *Atmos. Environ.* 14:1013–16
66. Williams RM. 1982. A model for the dry deposition of particles to natural water surfaces. *Atmos. Environ.* 16:1933–38
67. Pryor SC, Barthelmie RJ. 2000. Particle dry deposition to water surfaces: processes and consequences. *Mar. Pollut. Bull.* 41:220–31
68. Emerson EW, Katich JM, Schwarz JP, McMeeking GR, Farmer DK. 2018. Direct measurements of dry and wet deposition of black carbon over a grassland. *J. Geophys. Res. Atmos.* 123:12277–90
69. Warren SG, Wiscombe WJ. 1980. A model for the spectral albedo of snow. II: Snow containing atmospheric aerosols. *J. Atmos. Sci.* 37:2734–45
70. Flanner MG, Zender CS, Randerson JT, Rasch PJ. 2007. Present-day climate forcing and response from black carbon in snow. *J. Geophys. Res. Atmos.* 112:D11202
71. Koch D, Del Genio A. 2010. Black carbon semi-direct effects on cloud cover: review and synthesis. *Atmos. Chem. Phys.* 10:7685–96
72. Hansen J, Nazarenko L. 2004. Soot climate forcing via snow and ice albedos. *PNAS* 101:423–28
73. Bond TC, Streets DG, Yarber KF, Nelson SM, Woo JH, Klimont Z. 2004. A technology-based global inventory of black and organic carbon emissions from combustion. *J. Geophys. Res. Atmos.* 109:D14203
74. Hadley OL, Corrigan CE, Kirchstetter TW, Cliff SS, Ramanathan V. 2010. Measured black carbon deposition on the Sierra Nevada snow pack and implication for snow pack retreat. *Atmos. Chem. Phys.* 10:7505–13

75. Kaspari S, Skiles SM, Delaney I, Dixon D, Painter TH. 2015. Accelerated glacier melt on Snow Dome, Mount Olympus, Washington, USA, due to deposition of black carbon and mineral dust from wildfire. *J. Geophys. Res. Atmos.* 120:2793–807
76. Menon S, Koch D, Beig G, Sahu S, Fasullo J, Orlikowski D. 2010. Black carbon aerosols and the third polar ice cap. *Atmos. Chem. Phys.* 10:4559–71
77. Yasunari TJ, Tan Q, Lau KM, Bonasoni P, Marinoni A, et al. 2013. Estimated range of black carbon dry deposition and the related snow albedo reduction over Himalayan glaciers during dry pre-monsoon periods. *Atmos. Environ.* 78:259–67
78. Mahmood R, von Salzen K, Flanner M, Sand M, Langner J, et al. 2016. Seasonality of global and Arctic black carbon processes in the Arctic Monitoring and Assessment Programme models. *J. Geophys. Res. Atmos.* 121:7100–16
79. Schwarz JP, Gao RS, Fahey DW, Thomson DS, Watts LA, et al. 2006. Single-particle measurements of midlatitude black carbon and light-scattering aerosols from the boundary layer to the lower stratosphere. *J. Geophys. Res. Atmos.* 111:D16207
80. Stephens M, Turner N, Sandberg J. 2003. Particle identification by laser-induced incandescence in a solid-state laser cavity. *Appl. Opt.* 42:3726–36
81. Joshi R, Liu D, Nemitz E, Langford B, Mullinger N, et al. 2021. Direct measurements of black carbon fluxes in central Beijing using the eddy covariance method. *Atmos. Chem. Phys.* 21:147–62
82. Andrews T, Gregory JM, Webb MJ, Taylor KE. 2012. Forcing, feedbacks and climate sensitivity in CMIP5 coupled atmosphere-ocean climate models. *Geophys. Res. Lett.* 39:L09712
83. Bony S, Dufresne JL. 2005. Marine boundary layer clouds at the heart of tropical cloud feedback uncertainties in climate models. *Geophys. Res. Lett.* 32:L20806
84. Twomey S. 1974. Pollution and planetary albedo. *Atmos. Environ.* 8:1251–56
85. Ackerman AS, Toon OB, Taylor JP, Johnson DW, Hobbs PV, Ferek RJ. 2000. Effects of aerosols on cloud albedo: evaluation of Twomey's parameterization of cloud susceptibility using measurements of ship tracks. *J. Atmos. Sci.* 57:2684–95
86. Contini D, Donateo A, Belosi F, Grasso F, Santachiara G, Prodi F. 2010. Deposition velocity of ultrafine particles measured with the Eddy-Correlation Method over the Nansen Ice Sheet (Antarctica). *J. Geophys. Res. Atmos.* 115:D16202
87. Duan B, Fairall C, Thomson D. 1988. Eddy correlation measurements of the dry deposition of particles in wintertime. *J. Appl. Meteorol.* 27:642–52
88. Ibrahim M, Barrie L, Fanaki F. 1983. An experimental and theoretical investigation of the dry deposition of particles to snow, pine trees and artificial collectors. *Atmos. Environ.* 17:781–88
89. Nilsson ED, Rannik Ü. 2001. Turbulent aerosol fluxes over the Arctic Ocean: 1. Dry deposition over sea and pack ice. *J. Geophys. Res. Atmos.* 106:32125–37
90. Grönlund A, Nilsson D, Koponen IK, Virkkula A, Hansson ME. 2002. Aerosol dry deposition measured with eddy-covariance technique at Wasa and Aboa, Dronning Maud Land, Antarctica. *Ann. Glaciol.* 35:355–61
91. Gallagher M, Beswick K, Choularton T. 1992. Measurement and modelling of cloudwater deposition to a snow-covered forest canopy. *Atmos. Environ. A.* 26:2893–903
92. Macdonald KM, Sharma S, Toom D, Chivulescu A, Hanna S, et al. 2017. Observations of atmospheric chemical deposition to high Arctic snow. *Atmos. Chem. Phys.* 17:5775–88
93. Huang L, Gong SL, Jia CQ, Lavoue D. 2010. Importance of deposition processes in simulating the seasonality of the Arctic black carbon aerosol. *J. Geophys. Res. Atmos.* 115:D17207
94. Tammet H, Kimmel V, Israelsson S. 2001. Effect of atmospheric electricity on dry deposition of airborne particles from atmosphere. *Atmos. Environ.* 35:3413–19
95. Pryor SC, Barthelmie RJ, Larsen SE, Sørensen LL. 2017. Ultrafine particle number fluxes over and in a deciduous forest. *J. Geophys. Res. Atmos.* 122:405–22
96. Rannik Ü, Mammarella I, Aalto P, Keronen P, Vesala T, Kulmala M. 2009. Long-term aerosol particle flux observations part I: uncertainties and time-average statistics. *Atmos. Environ.* 43:3431–39
97. Mammarella I, Rannik Ü, Aalto P, Keronen P, Vesala T, Kulmala M. 2011. Long-term aerosol particle flux observations. Part II: Particle size statistics and deposition velocities. *Atmos. Environ.* 45:3794–805

98. Deventer MJ, von der Heyden L, Lamprecht C, Graus M, Karl T, Held A. 2018. Aerosol particles during the Innsbruck Air Quality Study (INNAQS): fluxes of nucleation to accumulation mode particles in relation to selective urban tracers. *Atmos. Environ.* 190:376–88
99. Jarvi L, Rannik Ü, Mammarella I, Sogachev A, Aalto PP, et al. 2009. Annual particle flux observations over a heterogeneous urban area. *Atmos. Chem. Phys.* 9:7847–56
100. Conte M, Contini D. 2019. Size-resolved particle emission factors of vehicular traffic derived from urban eddy covariance measurements. *Environ. Pollut.* 251:830–38
101. Pallozzi E, Guidolotti G, Mattioni M, Calfapietra C. 2020. Particulate matter concentrations and fluxes within an urban park in Naples. *Environ. Pollut.* 266:115134
102. Fares S, Savi F, Fusaro L, Conte A, Salvatori E, et al. 2016. Particle deposition in a peri-urban Mediterranean forest. *Environ. Pollut.* 218:1278–86
103. Ahlm L, Nilsson ED, Krejci R, Martensson EM, Vogt M, Artaxo P. 2009. Aerosol number fluxes over the Amazon rain forest during the wet season. *Atmos. Chem. Phys.* 9:9381–400
104. Chamberlain A. 1967. Transport of Lycopodium spores and other small particles to rough surfaces. *Proc. R. Soc. A Math. Phys. Eng. Sci.* 296:45–70
105. Clough W. 1975. The deposition of particles on moss and grass surfaces. *Atmos. Environ.* 9:1113–19
106. Wesely M, Hicks B, Dannevik W, Frisella S, Husar R. 1977. An eddy-correlation measurement of particulate deposition from the atmosphere. *Atmos. Environ.* 11:561–63
107. Garland J, Cox L. 1982. Deposition of small particles to grass. *Atmos. Environ.* 16:2699–702
108. Dollard G, Unsworth M. 1983. Field measurements of turbulent fluxes of wind-driven fog drops to a grass surface. *Atmos. Environ.* 17:775–80
109. Katen PC, Hubbe JM. 1985. An evaluation of optical particle counter measurements of the dry deposition of atmospheric aerosol particles. *J. Geophys. Res. Atmos.* 90:2145–60
110. Wesely M, Cook D, Hart R, Speer R. 1985. Measurements and parameterization of particulate sulfur dry deposition over grass. *J. Geophys. Res. Atmos.* 90:2131–43
111. Hicks B, Wesely M, Coulter R, Hart R, Durham J, et al. 1986. An experimental study of sulfur and NO_X fluxes over grassland. *Bound. Layer Meteorol.* 34:103–21
112. Gallagher M, Choularton T, Morse A, Fowler D. 1988. Measurements of the size dependence of cloud droplet deposition at a hill site. *Q. J. R. Meteorol. Soc.* 114:1291–303
113. Fowler D, Morse A, Gallagher M, Choularton T. 1990. Measurements of cloud water deposition on vegetation using a lysimeter and a flux gradient technique. *Tellus B Chem. Phys. Meteorol.* 42:285–93
114. Allen A, Harrison R, Nicholson K. 1991. Dry deposition of fine aerosol to a short grass surface. *Atmos. Environ. A.* 25:2671–76
115. Nemitz E, Gallagher MW, Duyzer JH, Fowler D. 2002. Micrometeorological measurements of particle deposition velocities to moorland vegetation. *Q. J. R. Meteorol. Soc.* 128:2281–300
116. Vong RJ, Vickers D, Covert DS. 2004. Eddy correlation measurements of aerosol deposition to grass. *Tellus B Chem. Phys. Meteorol.* 56:105–17
117. Connan O, Pellerin G, Maro D, Damay P, Hébert D, et al. 2018. Dry deposition velocities of particles on grass: field experimental data and comparison with models. *J. Aerosol Sci.* 126:58–67
118. Höfken KD, Gravenhorst G. 1982. Deposition of atmospheric aerosol particles to beech- and spruce forest. In *Deposition of Atmospheric Pollutants: Proceedings of a Colloquium Held at Oberursel/Taunus, West Germany, November 9–11, 1981*, ed. H-W Georgii, J Pankrath, pp. 191–94. Dordrecht, Neth.: Springer
119. Grosch S, Schmitt G. 1988. Experimental investigations on the deposition of trace elements in forest areas. In *Environmental Meteorology: Proceedings of an International Symposium Held in Wurzburg, F.R.G., September 29–October 1, 1987*, ed. K Grafen, pp. 201–16. Dordrecht, Neth.: D. Reidel Publ.
120. Waraghai A, Gravenhorst G. 1989. Dry deposition of atmospheric particles to an old spruce stand. In *Proceedings of the Meeting on Mechanisms and Effects of Pollutant-Transfer into Forests, Held in Oberurse/Taunus, F.R.G., November 24–25, 1988*, ed. H-W Georgii, pp. 77–86. Dordrecht, Neth.: Kluwer Acad. Publ.
121. Lorenz R, Murphy C. 1989. Dry deposition of particles to a pine plantation. *Bound. Layer Meteorol.* 46:355–66
122. Gallagher M, Beswick K, Duyzer J, Westrate H, Choularton T, Hummelshøj P. 1997. Measurements of aerosol fluxes to Speulder forest using a micrometeorological technique. *Atmos. Environ.* 31:359–73

123. Held A, Nowak A, Wiedensohler A, Klemm O. 2006. Field measurements and size-resolved model simulations of turbulent particle transport to a forest canopy. *J. Aerosol Sci.* 37:786–98
124. Pryor S. 2006. Size-resolved particle deposition velocities of sub-100 nm diameter particles over a forest. *Atmos. Environ.* 40:6192–200
125. Grönholm T, Launiainen S, Ahlm L, Mårtensson E, Kulmala M, et al. 2009. Aerosol particle dry deposition to canopy and forest floor measured by two-layer eddy covariance system. *J. Geophys. Res. Atmos.* 114:D04202
126. Gordon M, Staebler RM, Liggio J, Vlasenko A, Li SM, Hayden K. 2011. Aerosol flux measurements above a mixed forest at Borden, Ontario. *Atmos. Chem. Phys.* 11:6773–86
127. Zhang J, Shao Y, Huang N. 2014. Measurements of dust deposition velocity in a wind-tunnel experiment. *Atmos. Chem. Phys.* 14:8869–82
128. Deventer MJ, Held A, El-Madany TS, Klemm O. 2015. Size-resolved eddy covariance fluxes of nucleation to accumulation mode aerosol particles over a coniferous forest. *Agric. Forest Meteorol.* 214–215:328–40
129. Möller U, Schumann G. 1970. Mechanisms of transport from the atmosphere to the Earth's surface. *J. Geophys. Res.* 75:3013–19
130. Sehmel G, Sutter S. 1974. *Particle deposition rates on a water surface as a function of particle diameter and air velocity*. Rep. BNWL-1850, Battelle Pac. Northwest Labs, Richland, WA
131. Larsen SE, Edson J, Hummelshøj P, Jensen NO, De Leeuw G, Mestayer P. 1995. Dry deposition of particles to ocean surfaces. *Ophelia* 42:193–204
132. Gustafsson MER, Franzén LG. 1996. Dry deposition and concentration of marine aerosols in a coastal area, SW Sweden. *Atmos. Environ.* 30:977–89
133. Zufall MJ, Davidson CI, Caffrey PF, Ondov JM. 1998. Airborne concentrations and dry deposition fluxes of particulate species to surrogate surfaces deployed in southern Lake Michigan. *Environ. Sci. Technol.* 32:1623–28
134. Caffrey PF, Ondov JM, Zufall MJ, Davidson CI. 1998. Determination of size-dependent dry particle deposition velocities with multiple intrinsic elemental tracers. *Environ. Sci. Technol.* 32:1615–22
135. Petelski T. 2003. Marine aerosol fluxes over open sea calculated from vertical concentration gradients. *J. Aerosol Sci.* 34:359–71
136. Pryor S, Gallagher M, Sievering H, Larsen SE, Barthelmie RJ, et al. 2008. A review of measurement and modelling results of particle atmosphere–surface exchange. *Tellus B Chem. Phys. Meteorol.* 60:42–75
137. Zhang G, Zhang J, Liu S. 2007. Characterization of nutrients in the atmospheric wet and dry deposition observed at the two monitoring sites over Yellow Sea and East China Sea. *J. Atmos. Chem.* 57:41–57
138. Shi J-H, Zhang J, Gao H-W, Tan S-C, Yao X-H, Ren J-L. 2013. Concentration, solubility and deposition flux of atmospheric particulate nutrients over the Yellow Sea. *Deep Sea Res. II Top. Stud. Oceanogr.* 97:43–50
139. Calec N, Boyer P, Anselmet F, Amielh M, Branger H, Mailliat A. 2017. Dry deposition velocities of submicron aerosols on water surfaces: laboratory experimental data and modelling approach. *J. Aerosol Sci.* 105:179–92
140. Qi J, Yu Y, Yao X, Gang Y, Gao H. 2020. Dry deposition fluxes of inorganic nitrogen and phosphorus in atmospheric aerosols over the Marginal Seas and Northwest Pacific. *Atmos. Res.* 245:105076
141. Sehmel GA. 1973. Particle eddy diffusivities and deposition velocities for isothermal flow and smooth surfaces. *J. Aerosol Sci.* 4(2):125–38

Annual Review of
Physical Chemistry
Volume 72, 2021

Contents

Errata

An online log of corrections to *Annual Review of Physical Chemistry* articles may be found at http://www.annualreviews.org/errata/physchem